Pergamon

Journal of Structural Geology, Vol. 17, No. 6, pp. 765 to 775, 1995

0191-8141/95 $9.50 + 0.00

0191-8141(94)00110-3

Origin of the western Subbetic arc (South Spain): palaeomagnetic and structural evidence

JOHN PLATT, SIMON ALLERTON, ANDREW KIRKER and ELLEN PLATZMAN

Department of Earth Sciences, Oxford University, Oxford OX1 3PR, U.K.

(*Received* 9 *March* 1994; *accepted in revised form* 27 *September* 1994)

Abstract—An integrated structural and palaeomagnetic study in Late Cretaceous–Eocene rocks of the western Subbetic arc in the Betic Cordillera of southern Spain shows that the change in fold trend around the arc is significantly greater than the variation in primary magnetic declination. This suggests that the arcuate geometry is not primarily a consequence of differential rotation. The area has experienced a regional clockwise rotation of at least 40°, which was most probably imposed during oblique WNW-directed convergence along the southern Iberian margin in early Miocene time, before the arcuate structure was formed. Kinematic indicators associated with the arcuate folds and thrust traces are for the most part consistently WNW-directed, suggesting that the arc is not primarily a result of variations in the direction of tectonic transport. The arcuate structure was probably initiated without significant rotation by the WNW-directed indentation of the curved western end of the Alboran domain into the Iberian margin, and was then tightened, involving up to about 35° of further rotation in different segments of the arc. Finally, one sector in the arc was rotated anticlockwise by about 40° with respect to the rest of the region, reorientating the magnetic declinations, the fold trends, and the kinematic indicators. This rotation was associated with local sinistral shear.

INTRODUCTION

The Betic-Rif arc is one of the most tightly arcuate mountain chains in the world (Fig. 1). The Neogene thrust belts that form the External Zones of the arc swing through 180°, from a WSW-trend in the Subbetic Zone of southern Spain, through the south across the Straits of Gibraltar, to the east and even the east-northeast in the External Rif of Morocco. This geometry has invited various explanations in the past, including oroclinal bending of an originally straight convergent mountain chain between Africa and Europe (Carey 1955), deformation around a westward-driving Alboran microplate between Africa and Europe (Andrieux *et al.* 1971, Leblanc & Olivier 1984, Sanz de Galdeano 1990), and outwardly directed thrusting driven by the gravitational collapse of a region of high elevation centred on the present Alboran Sea (van Bemmelen 1969, Torres Roldán 1979, Platt & Vissers 1989). Observations of the orientation, magnitude and timing of deformation and rotation around the arc should in principle distinguish among these different explanations.

The Internal Zones of the Betic Cordillera and the Rif consist mainly of rocks deformed and metamorphosed in Late Cretaceous to early Miocene time, and represent the remains of an essentially pre-Neogene collisional mountain chain between Africa and Iberia. Similar rocks probably underlie much of the Alboran Sea, and the whole region, known collectively as the Alboran Domain, has played a critical role in the formation of the arcuate Neogene thrust belts around its margin. The boundary between the Alboran domain and the External Zones of the Betic–Rif arc, which we will refer to as the Internal/External Zone Boundary (IEZB), is the most important tectonic contact in the region, and in itself helps to define the arc. The nature of this boundary is somewhat controversial. The long WSW-trending segment in the Betic Cordillera has been described as a dextral strike-slip fault by Leblanc & Olivier (1984) and Sanz de Galdeano (1990), for example, but as a S-directed backthrust emplacing External Zone rocks over the Internal Zone by Garcia-Dueñas & Navarro-Vila (1976). Structural and kinematic work by Lonergan *et al.* (1993) demonstrate that in the eastern Betics the IEZB is a gently N-dipping backthrust with motion towards the south and southeast. In the region of the Gibraltar arc Balanyá & Garcia-Dueñas (1987) refer to the IEZB as the Gibraltar crustal thrust, presumably directed towards the west, but they suggest that it has been massively reactivated by S-directed extensional motion. In the southern part of the Rif Platzman *et al.* (1993) show that it is gently dipping S-directed thrust.

The External Zones of the Betic–Rif arc consist of a number of geologically separate segments, none of which can be followed all the way round the arc (Didon *et al.* 1967, Bourgois 1977). The Prebetic and Subbetic Zones of the Betic Cordillera consist of Mesozoic and Tertiary sediments deposited on the southern rifted margin of Iberia, and deformed by thin-skinned folding and thrusting during the Miocene (García-Hernandez *et al.* 1980, Banks & Warburton 1991, Blankenship 1992). The Subbetic as a whole trends west-southwest, heading out towards the Atlantic coast by Cadiz (Fig. 1), and only the internal part of the Subbetic swings around to form the arcuate structure that is the topic of this paper. In the western Betics the so-called Flysch Units appear structurally above the Subbetic, and in places lie tectonically above the Internal Zones. The Flysch Units become more important in the Gibraltar region and in the Rif. Traditionally they have been regarded as part of

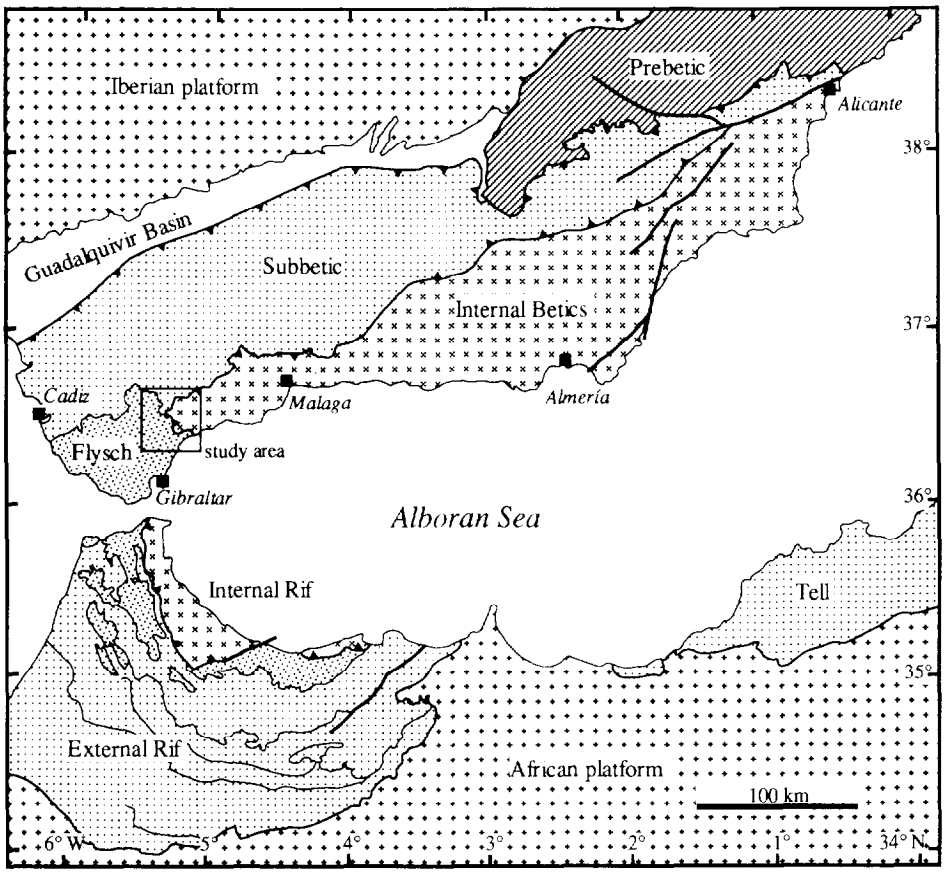

Fig. 1. Tectonic map of the Betic–Rif arc, showing location of the study area.

the Internal Zones, but in their tectonic characteristics (lack of basement involvement, lack of metamorphism, and Miocene age of deformation) they resemble the External Zones. In the Rif the Flysch Units lie structurally above the External Rif, which comprises Mesozoic and Tertiary sequences deposited on the rifted African margin (Wildi 1983, Favre *et al.* 1991).

Palaeomagnetic work in the Betic–Rif arc has demonstrated the importance of rotations about vertical axes. These are predominantly clockwise in the Betic Cordillera (Osete *et al.* 1989, Platzman & Lowrie 1992, Villalaín *et al.* 1992, Allerton *et al.* 1993); whereas in the Rif rotations in both senses occur, but anticlockwise rotations appear to be dominant (Platzman *et al.* 1993). These rotations have to be taken into account in structural analysis, and the possibility that fold trends and kinematic indicators have been rotated during or after formation must be considered.

The purpose of this paper is to present the results of an integrated structural and palaeomagnetic study of deformed Subbetic rocks adjacent to the IEZB in the western part of the Betic Cordillera, where the structural trend swings into the Gibraltar arc. The study was designed as a straightforward experiment to determine the degree of correlation between palaeomagnetically determined rotations, fold trends, and kinematic indicators, around a segment of the arc. This was intended both to constrain the extent to which structural data must be corrected for vertical-axis rotations, and to provide specific information on a critical sector of the arcuate structure. The study forms part of a programme of such investigations into the origin of the Betic–Rif arc as a whole (Allerton *et al.* 1993, Platzman *et al.* 1993, Lonergan *et al.* 1994).

GEOLOGICAL SETTING OF THE STUDY AREA

The Subbetic Zone comprises a shortened and thickened sequence of Mesozoic and Early Tertiary limestone and marl deposited on a series of platforms and basins forming the rifted southern margin of Iberia. In the western Betics (Fig. 2) it is overlain tectonically by the Gibraltar flysch units, which include thick sequences of predominantly Oligocene–early Miocene siliciclastic rocks (Didon 1969, Martín-Algarra 1987), and by the Internal Zones along the IEZB. Sandwiched along the IEZB is a thin sequence of highly deformed clastic rocks and marls of uncertain palaeogeographic affinity ranging in age up to early Miocene (Burdigalian) (Olivier 1984, Martín-Algarra 1987), which appear to constrain motion on the IEZB to early–middle Miocene time. The Subbetic is overlain by late Miocene (Tortonian) post-compressional sediments.

In the area round Gaucín the Subbetic closest to the IEZB contains a sequence of pink well-bedded marly limestones of Late Cretaceous–Eocene age (Fig. 2), known informally in Spanish as *capas rojas* (Martín-Algarra 1987). These rocks are ideal for the study presented here, in that: (1) they contain compact beds of

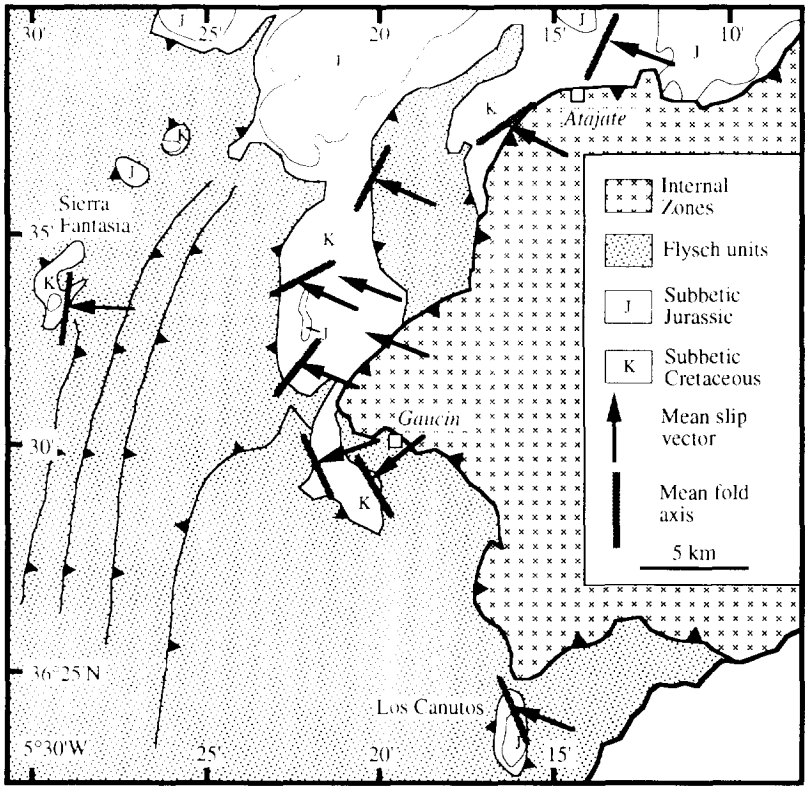

Fig. 2. Tectonic map of the westernmost Subbetics showing fold trends and kinematic vectors. Geology modified after Instituto Geológico y Minero de España (1987).

limestone with stable magnetic remanences suitable for palaeomagnetic work; (2) they are folded at a variety of scales, giving clear-cut structural trends as well as outcrops suitable for palaeomagnetic fold tests; and (3) they contain abundant calcite fibre-lineations on fault and bedding-plane-slip surfaces, as well as clear-cut sense of shear indicators. They therefore allow the measurement of structural, kinematic and palaeomagnetic data at the same location. The outcrop of *capas rojas* defines a belt that changes trend through about 90° as it enters the Gibraltar arc (Fig. 2). We also included two tectonic windows of Subbetic rocks within the outcrop area of the Gibraltar flysch units, as they appear to be part of the same belt of rocks.

STRUCTURAL ANALYSIS

The *capas rojas* in the study area forms a coherent but internally deformed sheet of rock lying stratigraphically above Early Cretaceous marl and massive Jurassic limestone, and tectonically overlain by flysch and by the rocks of the Internal Zones. It has a present structural thickness of several hundred metres, but its original stratigraphic thickness cannot be determined precisely. It contains abundant angular folds on scales ranging from 1 to 50 m, with chevron or kink geometries. Their trends swing from east-northeast to northwest around the belt (Figs. 2 and 4a); axial planes are steep, and the local sense of asymmetry (vergence) of the folds is variable, but is dominantly outwards with respect to the arc (i.e. NW-, W- or SW-vergent). Larger scale, possibly younger, open folds with roughly N–S trends are defined by the outcrop pattern of the Jurassic rocks in two tectonic windows (Los Canutos and Cerro Fantasia, Fig. 2), and in the Guadiaro river (south of the site B304/5 in Fig. 3). The rocks are also cut by numerous small faults, including reverse faults that may be W- or E-directed, sinistral and dextral strike-slip faults, and less common normal faults. The faults commonly contain gouge zones with well-developed gouge fabrics and Riedel shears, and linear indicators such as fibre-lineated calcite veins, solution grooves and wear grooves, which we used to determine the orientation and sense of slip. In addition, there has been extensive distributed slip along bedding planes and cleavage surfaces, indicated by the presence of fibre-lineated calcite veins. In most cases these minor slip surfaces show a clear kinematic relationship to local fold and thrust structures.

Because of the abundance of small-scale structural data, we collected information systematically at structural 'sites', with dimensions of the order of 100 m. At each site we attempted to collect a statistically significant number (normally more than 12) of kinematic measurements from each set of structures, and to establish the age relations among different sets of lineations, different sets of fractures, and among fracture sets and other structures such as folds or cleavage. Site locations were chosen partly to obtain regional coverage, and more specifically to obtain data close to major tectonic boundaries and from palaeomagnetic sites. The kinematic data are presented in Figs. 2, 4(b) and 5, and are summarized in Table 1.

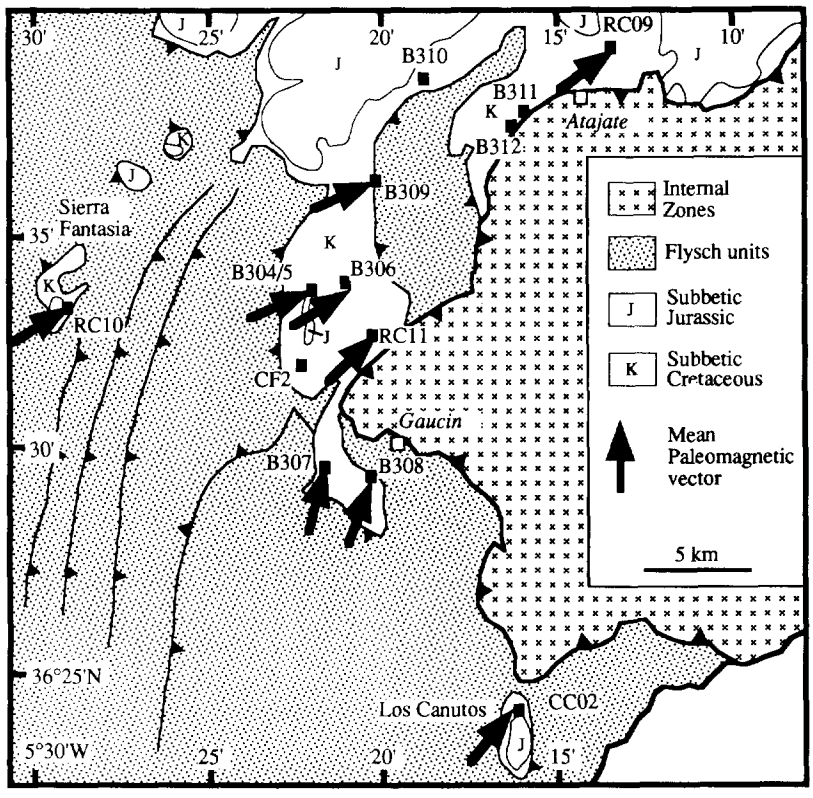

Fig. 3. Tectonic map of the westernmost Subbetics showing palaeomagnetic directions. Note that because the expected magnetic declination for the Late Cretaceous is very close to north, the declination values correspond to the amount of clockwise rotation relative to Iberia.

The oldest and by far the most important set of structures comprise the small-scale NW-, W- or SW-vergent folds and associated reverse faults, which have contributed to a substantial and pervasive deformation of the Cretaceous rock body. On a smaller scale, these structures are associated with a spaced pressure-solution cleavage and abundant microfaults and bedding-parallel slip surfaces marked by films of fibre-lineated calcite. These features are visible in nearly every outcrop we examined. In view of the proximity of the belt of *capas rojas* to the IEZB, it is reasonable to suppose that this set of structures broadly reflects the dominant sense of displacement along the boundary. The orientation of fold axes and kinematic indicators related to this deformation are presented in Figs. 4 and 5(a)–(d).

Intensive sinistral strike-slip faulting on a roughly N–S trend is present in several locations, most notably close to Gaucin at site B307 (Fig. 5f), and west of Atajate at site B311/2 (Fig. 5g). In neither case is it possible to map a discrete fault, but in both locations the local orientation of the IEZB may be affected by these shear zones. Minor dextral and sinistral faults with variable trends are present in many outcrops (e.g. Figs. 5e & h) but the data sets from individual locations are generally too small to make statistically viable statements about their orientations. These faults probably have several different origins. Roughly E–W-trending faults with dextral shear sense (e.g. Fig. 5h) may be transfer faults associated with the WNW-directed compressional deformation. Others may be conjugate to be main N–S-trending sinistral set.

We have observed some S-directed minor normal faults, particularly at site B310 (Fig. 5i). This deformation is not widespread, and is the only evidence we have found to support the hypothesis of Balanya & Garcia-Dueñas (1987) that the region has been affected by substantial S-directed extensional deformation.

PALAEOMAGNETIC ANALYSIS

Sampling and measurement

To investigate the rotational component of the deformation of this region, 11 sites were sampled for measurement of palaeomagnetic properties. Palaeomagnetic sites were required to show clear bedding, a relative coherence with the large-scale structure, a minimum of internal deformation, and to cover a sufficient time interval to average out secular variation. Sites with low structural dips were sampled preferentially, although occasionally steeply inclined units were chosen where other suitable palaeomagnetic material is absent.

Sampling involved drilling standard 2.5 cm diameter cores, oriented using both sun and magnetic compasses. Typically, between 9 and 16 cores were taken at each site, and between one and three samples were obtained from each core. Magnetizations were measured in Oxford on a C.C.L. cryogenic magnetometer. Standard measurement procedure involved stepwise thermal magnetisation until no measurable signal could be identified. Initially, bulk susceptibility was measured

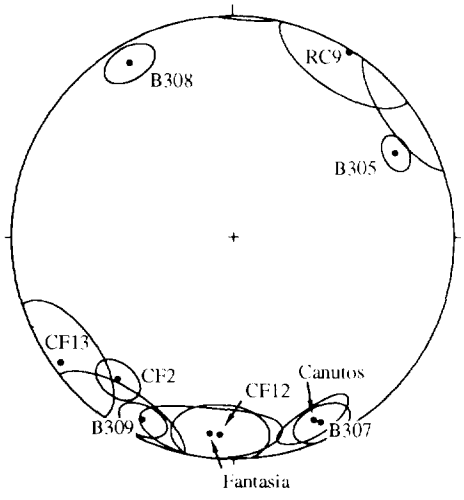

a. Mean fold axes

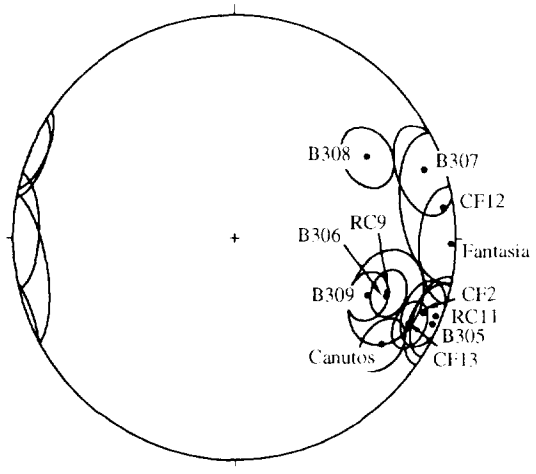

b. Mean lineations

Fig. 4. Equal area projections showing: (a) mean fold axes from the various sites, with Fisher circles of confidence about the means; and (b) mean kinematic vectors.

after each demagnetization step to monitor growth of magnetic minerals during heating, but where no significant change was noted, this was discontinued. Components were analysed on orthogonal plots using a least squares routine. IRM acquisition and demagnetization experiments were completed on selected samples to investigate the magnetic mineralogy.

Magnetic mineralogy

To investigate the magnetic mineralogy of the samples stepwise IRM acquisition and thermal demagnetization of two-component IRM experiments (Lowrie 1990) were completed. Figure 6 shows the results of one such experiment. The IRM acquisition curve shows a steep, linear gradient up to about 0.1 T, and a shallower gradient above this. This suggests the presence of two phases, one which saturates below 0.5 T, and a second which has not completely saturated by 0.8 T. Thermal demagnetization of a two-component IRM was applied to determine the unblocking temperature spectrum of a low coercivity phase (below 0.15 T) and a high coercivity phase (between 0.5 T and 0.8 T). The low coercivity phase is progressively removed by thermal demagnetization, and completely disappears by about 580°C. This phase is probably carried by (titano)magnetites. The high coercivity phase (between 0.15 T and 0.8 T) is progressively unblocked at temperatures up to about 650°C, although less than 1% remains above 580°C. This component is probably carried by pigmentary hematite (Collinson 1974).

Palaeomagnetic components

A poorly defined low-temperature component can be isolated below about 300°C. This component fails fold tests and scatters about the present dipole field direction; it is interpreted as a recent overprint.

The majority of the samples show a stable remanence on stepwise thermal demagnetization between about 300°C and 600°C (Fig. 7a, Table 2). Comparison with the acquisition and demagnetization of IRM experiments suggest that this component is carried by both magnetite and hematite, which have similar unblocking temperature spectra in this temperature range.

Two outcrop-scale folds were sampled at sites B304/5 and B308 to test the relative age of the magnetization. Both folds belong to the main set of small-scale structures associated with thrusting. The fold sampled at site B304/5 is a symmetric anticline with a vertical axial plane. The fold axis plunges at 19° to 074. The fold sampled at site B308 is an asymmetric anticline, vergent to the west, and plunging gently (7°) to the north. Bedding corrections that include a correction for the plunge of the folds have been applied to these data. The stable component from these sites pass both McElhinney (1964) and McFadden (1990) fold tests (see Table 3). These results indicate that this component predates the folding in Miocene times.

After a bedding correction has been applied, the sites exhibit normal, reversed and mixed polarities. In the one site that contains both polarities, the samples containing normal directions are confined to the bottom of the section (12 samples) and those containing reversed directions (three samples) to the top.

The high-temperature component is well defined in samples with a normal remanence, but in those carrying a reversed remanence, this component is often obscured by the lower temperature component (e.g. Fig. 7b). This is reflected in the intra-site precision: for normal and mixed polarity sites, precision is high, with $\alpha_{95} \leq 10°$. In contrast, values of α_{95} for reversed sites are all greater than 13°.

One site (B311) yields an apparently normal component that has poor precision, and a declination about 180° different to neighbouring sites. We believe that the stable component is heavily contaminated by the low-temperature component at this site, and that it represents a poorly isolated reversed direction.

Site RC11 has reasonable intra-site precision, but an anomalously shallow reversed inclination. Inspection of the demagnetization diagrams suggests that the com-

Table 1. Summary of structural data

Locality	Mean fault plane	Mean slip vector	Shear sense	Mean fold axis
CF2	54/136	15/063	Sinistral	
	22/180	11/112 ± 9.3	Thrust WNW	18/219 ± 7.6
B304-5	23/160	3/114 ± 11.5	Thrust WNW	18/063 ± 5.8
B306	35/161	29/111 ± 14.6	Thrust WNW	
B307	32/077	10/071 ± 13.1	Thrust WSW	8/154 ± 8.5
	82/104	14/015	Sinistral	
B308	31/049	31/050 ± 10.3	Thrust WSW	09/329 ± 7.9
B309	38/122	35/113 ± 8.2	Thrust WNW	09/207 ± 7.3
B310	19/163	05/082 ± 20.5	Thrust W	12/184 ± 14.2
CF12	51/167	49/201	Normal	
B311-312	77/123	06/032	Sinistral	
CF13	69/206	13/293	Dextral	
	43/145	13/136 ± 7.3	Thrust WNW	4/234 ± 18.8
RC9	33/140	27/110 ± 7.6	Thrust WNW	3/206 ± 17
RC11		3/114 ± 11.3	Thrust WNW	
Fantasia		3/093 ± 15.6	Thrust W	12/187 ± 21
Canutos		19/126 ± 8.8	Thrust WNW	11/156 ± 12

ponents at this site are poorly defined. There is sufficient variation in bedding at the site to make a great circle analysis appropriate (Halls 1976).

The stable components are displayed in Fig. 3. We have rejected sites B311 and B312 because they have poor intra-site precisions as indicated by α_{95} values $> 20°$ (see Table 2). The high-temperature components from site B310 are highly contaminated by the low-temperature component, and fall on a girdle between the low-temperature component and the (imperfectly defined) high-temperature component. The best mean direction that can be determined has an anomalously shallow inclination; this site has also not been included in further discussions of the data.

The magnetic mineralogical studies suggest that the carriers are hematite and magnetite, in varying proportions. The fold tests suggest that the stable high-temperature components were acquired before the Miocene folding episode, and should be useful for identifying tectonic rotations associated with and post-dating folding. They may also record earlier rotations that may have occurred between the acquisition of the magnetization, and the folding.

RELATIONS AMONG FOLD TRENDS, KINEMATICS AND PALAEOMAGNETIC DECLINATIONS

Two key questions must be addressed in any study of the geometry and kinematics of formation of a structure such as the Gibraltar arc.

(1) To what extent was the formation of the arcuate structure accompanied by differential rotation of rock bodies?

(2) To what extent have structural features such as fold trends and kinematic indicators been rotated from their original orientations?

The palaeomagnetic measurements demonstrate that there have been large clockwise rotations, as is the case elsewhere in the Betic Cordillera. The Late Cretaceous magnetic declination for stable Iberia is 358° (Westphal *et al.* 1986) so if the magnetic remanances are primary, the declinations plotted in Fig. 3 give a direct indication of the vertical-axis rotations. A problem that affects the structural interpretation of these data, however, is that the measured rotations are relative to an external reference frame (Iberia in this case), and do not in themselves carry information about the relationship between the rotations and the deformation in the surrounding rocks. To answer the questions posed above, therefore, we need to establish whether there is a relationship between the variations in rotation and the orientations of the structures, bearing in mind that both structural elements and palaeomagnetic remanences exhibit a natural scatter. For this reason we start our discussion by trying to establish the general level of correlation among the different measurements. Plots of fold trends and kinematic indicators against palaeomagnetic declinations are presented in Figs. 8 and 9, and of fold trend against kinematic direction in Fig. 10. The error bars shown on the points are 95% confidence intervals on the mean directions determined from Fisher statistics.

All three plots show a fairly large amount of uncorrelated scatter, but some provisional conclusions can be drawn.

(i) There appears to be some correlation between fold trends and palaeomagnetic declinations, with a slope significantly greater than 1 (Fig. 8).

(ii) There also appears to be a correlation between kinematic indicators and palaeomagnetic declinations, defined by two clusters, with a slope of about 1 (Fig. 9).

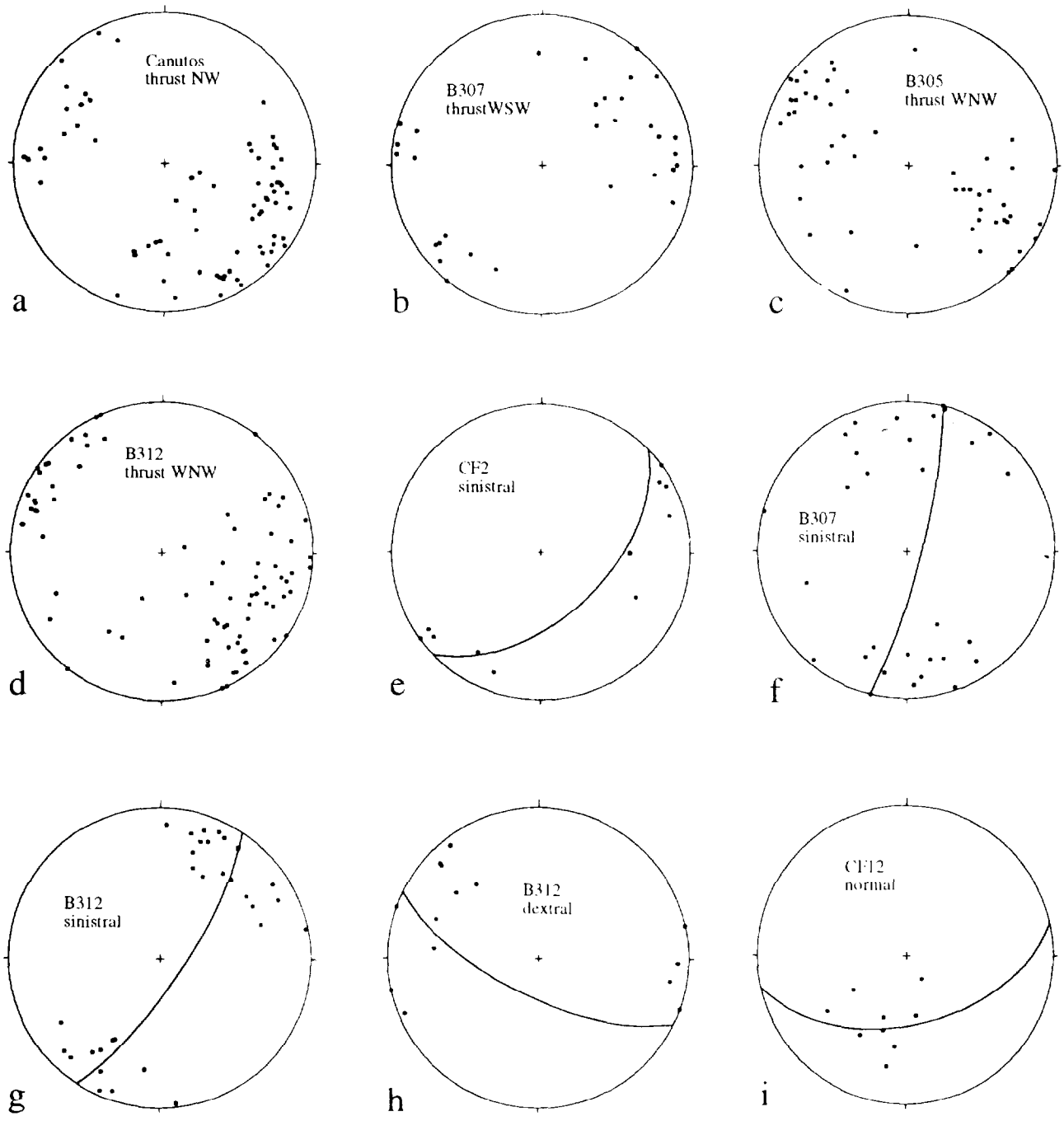

Fig. 5. Equal area projections showing kinematic data from selected sites. Mean fault planes are shown for strike-slip and normal indicators.

(iii) There is little correlation between fold trends and kinematic indicators: the slope of the correlation line is low, and the correlation coefficient is small (0.4, Fig. 10).

Inspection of Fig. 9 shows that the slope of the plot is controlled entirely by two locations that differ significantly from the rest. These are sites B307 and B308, located close to each other on the south side of the sharp promontory in the IEZB by Gaucin (Fig. 3). They show relatively low palaeomagnetic declinations (about 20°), NNW-trending folds, and SW-directed kinematic indicators. These two sites are potentially very important, as they lie at the extreme anticlockwise end of the range in all three measurements. It is not clear from Fig. 9, however, that conclusions based on these two sites would be supported by the remainder of the data. It is therefore worth excluding these two observations from consideration for the moment and examining the data without them.

Excluding sites B307 and B308, Fig. 9 shows virtually no correlation between kinematic vectors and magnetic declinations. The majority of the kinematic means lie in a fairly narrow band between 290° and 305°, and show no dependence on the amount of rotation. The consistency in orientation of the kinematic indicators is brought out even more clearly by the summary plot of the data in Fig. 4(b) and by the map (Fig. 2). This consistency suggests (but does not prove) that the lineations formed after the

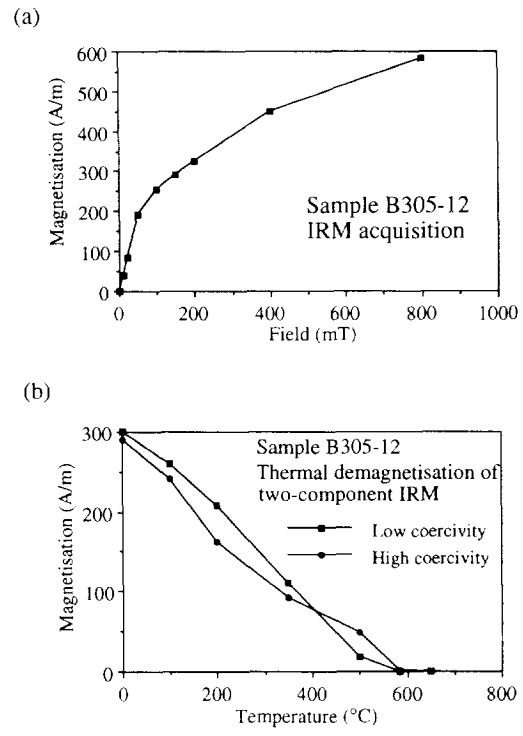

Fig. 6. (a) Example of an IRM acquisition experiment for sample B305-12. (b) Thermal demagnetization of two-component IRM for sample B305-12. Low coercivity phase is below 0.15 T and high coercivity phase is between 0.15 T and 0.8 T.

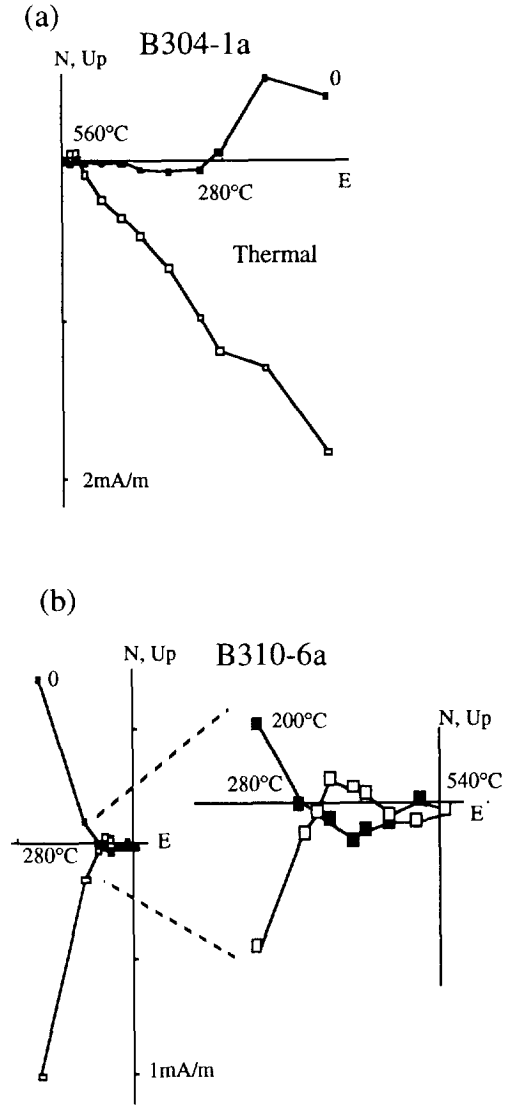

Fig. 7. Typical stepwise thermal demagnetization behaviour for Upper Cretaceous *capas rojas* facies samples: orthogonal vector diagrams (in situ; open symbols represent points in vertical plane; closed symbols, points in horizontal plane). (a) Sample B304-1a, with a normal high-temperature component. (b) Sample B310-6a, with a reversed high-temperature component. Note that the normal component is better defined than the reversed component.

differential rotations had occurred. There is, however, no constraint from the plot on their timing relative to the large overall rotation.

Excluding sites B307 and B308, the fold/declination plot (Fig. 8) is significantly steeper. The steepness of the slope (more than 2) suggests that the arcuate structure as a whole was not primarily a consequence of differential rotation. Of the 87° variation in fold trend, only 35° can be attributed to differential rotation around the arc. This leaves at least 40° (the rotation of the most southerly site at Canutos) of consistent clockwise rotation, which occurred independently of (presumably either before or after) the formation of the arcuate structure.

Excluding sites B307 and B308 from the plot of fold trend against kinematic direction (Fig. 10) further weakens the correlation in this plot. This reflects the fairly high degree of consistency of the kinematic indicators around the arc. In view of our field observations, which suggest that the kinematic indicators in any given area formed in close association with the local folds and thrusts, this lack of correlation of the orientations implies that the variation in fold trend was not caused by spatial variations in the direction of tectonic transport or of crustal shortening.

We must now consider the data from site B307 and B308, which we have omitted from the discussion so far. There is a significant difference in the declination and the kinematic indicators from these sites compared with all the other sites (Fig. 8). The difference is less obvious for the fold trends, because the Canutos site, which lies furthest south around the arc, has a similar trend. Canutos, however, has a declination and kinematic vector mean that fall within the group of all the other sites. If we compare the means for all three variables from B307 and B308 with the means for all the other sites, the differences are 38° in declination, 48° in kinematic direction, and 52° in fold trend. This seems to suggest quite strongly that there has been at least 40° differential rotation between the location of B307 and B308 and the rest of the area after the minor folds and the kinematic indicators had formed. This is a quite different conclusion from that based on the remainder of the data, and suggests that at least two different processes have contributed to the present structural geometry. It is significant that sites B307 and B308 lie in a region of intense sinistral shear (Fig. 5f). This provides a possible mechanism for late anticlockwise rotation of this area.

The preceding discussion, albeit rather tortuous, can

Table 2. Mean site data for the high-temperature magnetic component in *capas rojas* limestones

Site	Before correction				After correction							Bedding		Grid Ref.	
	D(°)	I(°)	k	α_{95}	D(°)	I(°)	k	α_{95}	N	n	n_r	Dip	Direction	East	North
B304	089	54	125	4	062	35	125	4	11	11	0	36	012	2881	0496
B305	024	25	70	5	074	46	70	5	11	11	0	74	158	2881	1496
B306	047	12	12	16	059	22	12	16	8	8	8	38	158	2904	0504
B307	040	28	15	10	016	53	16	10	15	15	3	41	259	2889	0433
B308	015	45	4	27	021	45	22	10	11	11	0	24	044	2899	0433
B309	029	47	20	10	067	50	20	10	11	11	0	32	143	2912	0537
RC09	057	50	72	6	055	42	90	5	10	10	0	11	022	3001	0587
RC10	027	34	27	9	059	40	38	8	12	11	0	44	136	2767	0479
RC11*	008	49	137	4	047	30	31	9	12	10	10	19	214	2902	0490
CC02	039	62	155	4	039	51	156	4	11	9	0	20	045	2965	0328
B310	090	−16	3	31	077	3	22	13	11	7	7	18	175	2942	0579
B311	270	16	245	64	243	48	4	40	6	6	0	10	336	2974	0576
B312	023	18	7	24	026	37	7	25	8	7	7	19	201	2974	0576

Directions are presented in normal polarity after bedding correction. N = total number of samples. n = number of samples in statistics. n_r = number of reversed polarity samples. α_{95} = radius of 95% circle of confidence about mean direction. k = dispersion parameter. Bedding is specified by dip and dip direction. Site locations are given as grid references from the IGME (Instituto Geológico y Minero de España) geological sheets 1064 and 1072. Sites CC02 and RC09 are from Platzman & Lowrie (1992). The last three sites have α_{95} greater than 20° or have anomalous inclinations, and have therefore been rejected (see text for explanation).

*RC11 corrected high-temperature component was calculated using intersecting great circles (Halls 1976). The 'before correction' direction is the low-temperature component, which is close to the present field direction; this component is used for the great-circle calculation.

Table 3. Results of palaeomagnetic fold tests

Site	Before			After				McElhinney (1964)			McFadden (1990)		
	Dec.	Inc.	k	Dec.	Inc.	k	N	k_{max}/k_{min}	Significance	CV	Before	After	Significance
B304/5	049	44	7.7	067	40	51.9	22	6.7	+ >99%	1.70	1.80	1.17	+ >95%
B308	015	45	3.9	021	45	21.8	11	5.6	+ >99%	1.70	1.95	0.13	+ >99%

Mean direction before and after application of a bedding correction. k = dispersion parameter. McElhinney (1964) fold-test parameter is k_{max}/k_{min}. McFadden (1990) test parameters: CV = critical value of test parameter at 95% confidence, and test parameters before and after tectonic correction. For McFadden, if test parameter > CV, then there is a correlation between tectonic correction and magnetic direction, and fold test is not significant. Results of tests are indicated as follows: negative (−) is magnetization acquired after folding, positive (+) is magnetization acquired before folding. Significance is expressed relative to a % confidence factor; <95% confidence is not considered significant.

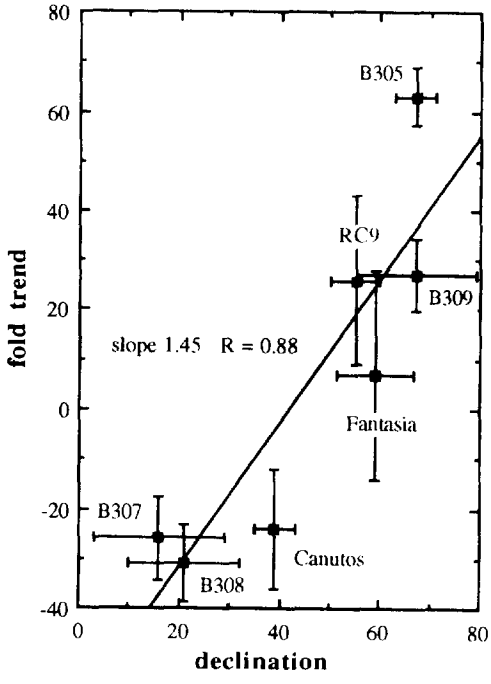

Fig. 8. Correlation plot of fold trends against palaeomagnetic declinations. In Figs. 8–10, error bars indicate the diameter of the Fisher circle of confidence about the mean for each variable. Slopes and correlation coefficients are indicated on each plot. Note that because the expected magnetic declination for the Late Cretaceous is very close to north, the declination values correspond to the amount of clockwise rotation relative to Iberia.

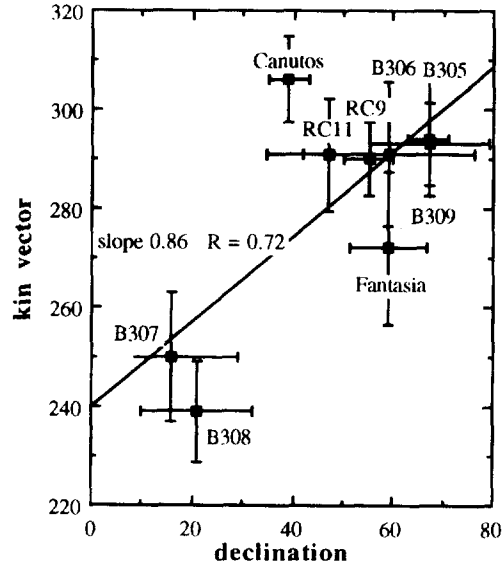

Fig. 9. Correlation plot of kinematic indicators against palaeomagnetic declinations.

be summarized in terms of the following four phenomena.

(1) The rocks of the region have experienced consistent clockwise rotation through at least 40°, independently of the formation of the arcuate structure. This

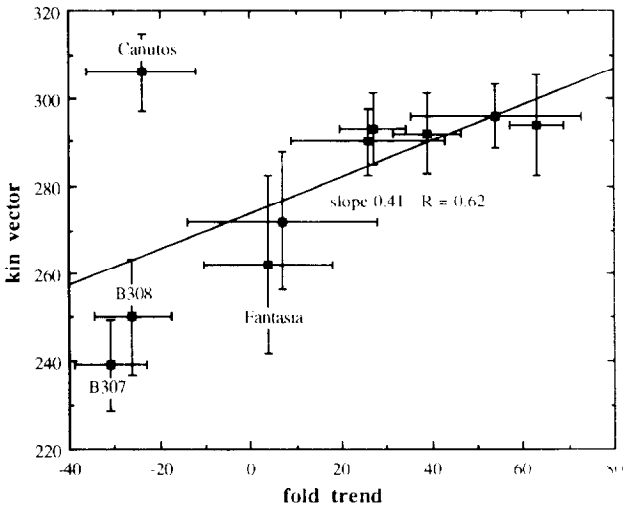

Fig. 10. Correlation plot of fold trends against kinematic indicators.

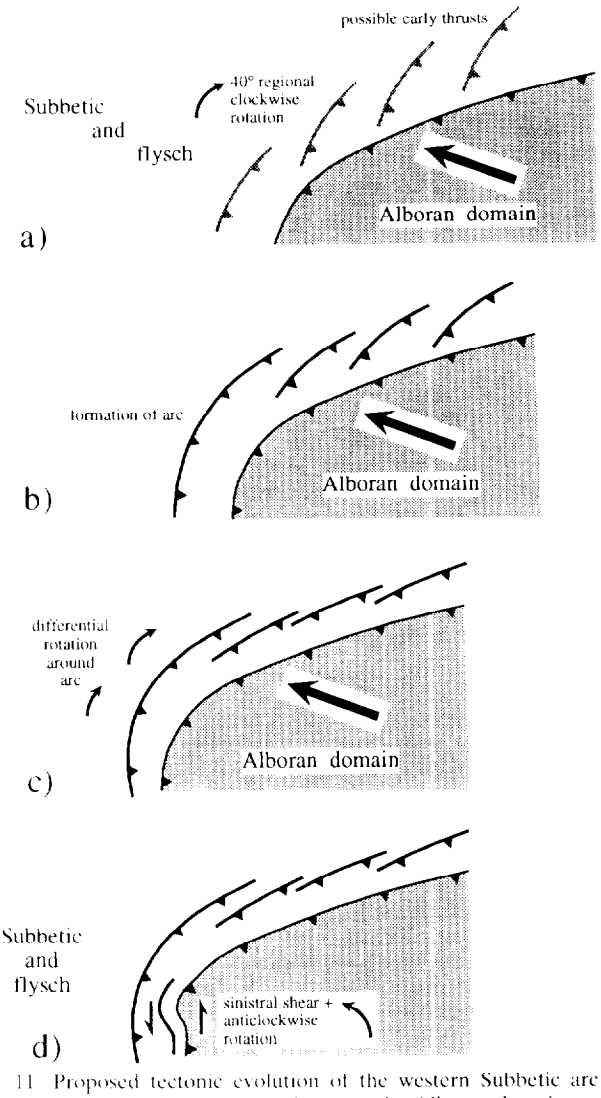

Fig. 11. Proposed tectonic evolution of the western Subbetic arc. (a) Dextrally oblique convergence between the Alboran domain and the Iberian margin early in Miocene time caused clockwise rotations. (b) The arcuate structure formed during indentation of the curved margin of the Alboran domain, without significant differential rotation. (c) Differential rotation was associated with tightening of the arc. (d) Sinistral strike-slip faulting in the Gaucin area caused local anticlockwise rotation of folds and kinematic indicators.

rotation could in principle have been imposed on the whole region as a block, or it could have been imposed as a series of coordinated rotations of smaller tectonic fragments. It could have occurred at any time relative to the other phenomena listed here.

(2) An arcuate pattern of folds and thrust traces was imposed on the area in approximately its present form: it was not formed primarily by differential rotation and bending of previously formed linear trends. The relative consistency of the kinematic indicators also suggests that it was not formed as a consequence of variations in the direction of thrusting or tectonic shortening.

(3) There has been some 35° of differential rotation around the arc, which has accentuated the arcuate geometry.

(4) Subsequent to the formation of the arc, the folds, and the lineations, there was a local anticlockwise rotation of the region immediately south of Gaucin (sites B307 and B308).

The relative timing of the regional clockwise rotation, and the causes of these four phenomena, are not constrained by the measurements, and must be discussed further in terms of the geological constraints.

The consistent part of the rotation history (phenomenon 1), consisting of clockwise rotation through at least 40° and possibly as much as 70°, could in principle have been imposed at any time. If it occurred after the folding and thrusting, however, the original thrusting direction indicated by the kinematics would have been towards the southwest. This seems incompatible with the regional tectonic setting, or with the overall evidence for approximately WNW–NW-convergence in the external Betic Cordillera as a whole (Guezou *et al.* 1991, Lonergan *et al.* 1994). It is also difficult to see why such a large regional clockwise rotation should have been associated with the formation of the arcuate structure itself. It seems most likely, therefore, that it occurred before the arcuate structure was imposed. We suggest that it was related to the initial stages of dextrally oblique convergence between the Alboran domain and the Iberian margin early in Miocene time (Fig. 11a). The lack of distinguishable folding or other small-scale deformation related to this phase of rotation may suggest that it occurred at the time thrusting started, when the sediments were cold and under no overburden. The Cretaceous rocks may have been carried passively on large rotating thrust slabs of massive Jurassic limestone, which in turn moved on a carpet of Triassic evaporites and shales.

The formation of the arcuate structure itself (phenomenon 2) is most plausibly related to the present geometry of the margin of the Alboran domain, which swings from an ENE to a N–S trend in the area. The curvature of the Alboran margin may have been accentuated in early Miocene time as a result of anticlockwise rotations in its westernmost segment (Platzman *et al.* 1993), to create a N–S-trending sector. WNW-convergence between this curved margin and the Subbetic provides a mechanism for initiating folds and thrust traces in an arcuate form,

in association with a consistent direction of thrusting, and without large differential rotations (Fig. 11b). Continued west-northwest motion of the Alboran domain would, however, generate a component of dextral shear on the ENE-trending part of the margin, which would tend to rotate the rocks and the developing structures further. This provides a mechanism for the differential rotation associated with tightening of the arc (phenomenon 3, Fig. 11c). Sinistral shear in the Gaucin area at a late stage, perhaps associated with a change to a more northerly direction of convergence, caused local anticlockwise rotation of folds and kinematic indicators (phenomenon 4, Fig 11d).

CONCLUSIONS

(1) The arcuate geometry of the folds and thrust traces in the western Subbetic is not primarily a consequence of differential rotation.

(2) Formation of the arcuate structure was not related to significant changes in the direction of tectonic transport or of crustal shortening, but was probably a consequence of WNW-directed indentation of the curved margin of the Alboran domain. Folds formed in a range of orientations around this curved margin while convergence and thrusting continued in a fairly consistent direction.

(3) A major part (at least 40°) of the clockwise rotation experienced by the Subbetic occurred independently of, and probably before, the imposition of the arcuate structure. This may have been the result of dextrally oblique convergence before the Alboran domain developed such a strongly curved western termination. Differential rotations of up to 35° were associated with the development and tightening of the arc. Additional rotation, apparently in an anticlockwise sense associated with sinistral shear, took place after formation of the main fold and thrust geometry.

Acknowledgements—This study was supported by NERC grant GR3/7125. We thank Buffy McClelland and an anonymous reviewer for constructive comments.

REFERENCES

Allerton, S., Lonergan, L., Platt, J. P., Platzman, E. S. & McClelland, E. 1993. Palaeomagnetic rotations in the eastern Betic Cordillera, southern Spain. *Earth & Planet. Sci. Lett.* **119**, 225–241.

Andrieux, J., Fontboté, J. M. & Mattauer, M. 1971. Sur un modèle explicatif de l'Arc de Gibraltar. *Bull. Sci. géol. Fr.* **7**, 115–118.

Balanyá, J. C. & García-Dueñas, V. 1987. Les directions structurales dans le Domaine d'Alboran de part et d'autre du Détroit de Gibraltar. *C. r. Acad. Sci. Paris* **304**, 929–932.

Banks, C. J. & Warburton, J. 1991. Mid-crustal detachment in the Betic system of southern Spain. *Tectonophysics* **191**, 275–289.

Blankenship, C. L. 1992. Structure and palaeogeography of the External Betic Cordillera, southern Spain. *Mar. Petrol. Geol.* **9**, 256–264.

Bourgois, 1977. S'une etape geodynamique majeure dans la genese de l'Arc de Gibraltar: L'hispanisation des flysch rifains au Miocène inférieur. *Bull. Soc. géol. Fr.* **12**, 1115–1119.

Carey, S. W. 1955. The orocline concept in geotectonics. *Proc. R. Soc. Tasmania* **89**, 255–288.

Collinson, D. W. 1974. The role of pigment and specularite in the remanent magnetism of red sandstones. *Geophys. J. R. Astron. Soc.* **38**, 253–274.

Didon, J. 1969. Etude géologique du Campo de Gibraltar (Espagne méridionale). Thesis, University of Paris, France.

Didon, J., Durand-Delga, M. & Kornprobst, J. 1967. Homologies géologiques entre les deux rives du détroit de Gibraltar. *Bull. Soc. géol. Fr.* **7**, 77–105.

Favre, P., Stampfli, G. & Wildi, W. 1991. Jurassic sedimentary record and tectonic evolution of the northwestern corner of Africa. *Palaeogeogr., Palaeoclimatol., Palaeoecol.* **87**, 53–73.

García-Hernández, M., López-Garrido, A. C., Rivas, P., Sanz de Galdeano, C. & Vera, J. A. 1980. Mesozoic palaeogeographic evolution of the external zones of the Betic Cordillera. *Geologie Mijnb.* **59**, 155–168.

García-Dueñas, V. & Navarro-Vila, F. 1976. Alpujarrides, Malaguides et autres unités allochtons au Nord de la Sierra Nevada (Cordilleres Bétiques, Andalousie). *Bull. Soc. géol. Fr.* **18**, 641–648.

Guezou, J. C., Frizon de Lamotte, D., Coulon, M. & Morel, J-L. 1991. Structure and kinematics of the Prebetic nappe complex (southern Spain): definition of a "Betic Floor Thrust" and implications in the Betic-Rif orocline. *Annls Tectonicae* **5**, 32–48.

Halls, H. C. 1976. A least squares method to find a remanence direction from converging remagnetization circles. *Geophys. J. R. Astro. Soc.* **45**, 297–304.

Instituto Geológico y Minero de España. 1987. Mapa geologico de España. 1:50,000. Cortes de la Frontera (1064).

Leblanc, D. & Olivier, P. 1984. Role of strike-slip faults in the Betic–Rifian Orogeny. *Tectonophysics* **101**, 345–355.

Lonergan, L., Platt, J. P. & Gallagher, L. 1994. The Internal External Zone Boundary in the eastern Betic Cordillera, SE Spain. *J. Struct. Geol.* **16**, 175–188.

Lowrie, W. 1990. Identification of ferromagnetic minerals in a rock by coercivity and unblocking temperature properties. *Geophys. Res. Lett.* **17**, 159–162.

Martin-Algarra, A. 1987. Evolucion geológica Alpina del contacto entre las zonas internas y las zonas externas de la Cordillera Bética. Thesis, University of Granada, vols 1 & 2.

McElhinney, M. W. 1964. Statistical significance of the fold test in palaeomagnetism. *Geophys. J. R. Astro. Soc.* **8**, 338–340.

McFadden, P. L. 1990. A new fold test in palaeomagnetic studies. *Geophys. J. Int.* **103**, 163–169.

Olivier, P. 1984. Evolution de la limite entre zones internes et zones externes dans l'Arc de Gibraltar. Thesis, University of Toulouse, France.

Osete, M. L., Freeman, R. & Vegas, R. 1989. Preliminary palaeomagnetic results from the Subbetic Zone, (Betic Cordillera, southern Spain): kinematic and structural implications. *Phys. Earth & Planet. Interiors* **52**, 283–300.

Platt, J. P. & Vissers, R. L. M. 1989. Extensional collapse of thickened continental lithosphere: a working hypothesis of the Alboran Sea and the Gibraltar arc. *Geology* **17**, 540–543.

Platzman, E. & Lowrie, W. 1992. Palaeomagnetic evidence for rotation of the Iberian Peninsula and the external Betic Cordillera, southern Spain. *Earth & Planet. Sci. Lett.* **108**, 45–60.

Platzman, E. S., Platt, J. P. & Olivier, P. 1993. Palaeomagnetic rotations and fault kinematics in the Rif arc of Morocco. *J. geol. Soc. Lond.* **150**, 707–718.

Sanz de Galdeano, C. 1990. Geologic evolution of the Betic Cordilleras in the Western Mediterranean, Miocene to present. *Tectonophysics* **172**, 107–119.

Torres-Roldán, R. 1979. The tectonic subdivision of the Betic Zone (Betic Cordilleras, Southern Spain): Its significance and one possible geotectonic scenario for the westernmost Alpine belt. *Am. J. Sci.* **279**, 19–51.

van Bemmelen, R. W. 1969. Origin of the western Mediterranean Sea. *Geologie Mijnb.* **26**, 13–52.

Villalain, J. J., Osete, M. L., Vegas, R. & García-Dueñas, V. 1992. Nuevos resultados paleomagnéticos en el Subbético Interno, implicaciones tectónicas. *Actas de las sesiones científicas, III Congreso Geologico de España* **1**, 308–312.

Westphal, M., Bazhenov, M. L., Lauer, J. P., Pechersky, D. M. & Sibuet, J. C. 1986. Palaeomagnetic implications on the evolution of the Tethys belt from the Atlantic ocean to the Pamirs since the Triassic. *Tectonophysics* **123**, 37–82.

Wildi, W. 1983. Le chaine tello-rifaine (Algérie, Maroc, Tunisie): Structure, stratigraphie et évolution du Trias au Miocène. *Revue de geologie dynamique et géographie physique* **24**, 201–297.